Scholar Publishing Group
International Journal of Engineering Technology and Construction
https://doi.org/10.38007/IJETC.2022.030202
ISSN 2789-7176 Vol. 3, Issue 2: 14-30

# *Market Development and Prospects of Farmland Irrigation Remote Sensing Monitoring Technology*

**Turiman Bin Suandi***

*Universiti Putra Malaysia, Malaysia*

**corresponding author*

***Keywords:*** Remote Sensing, Irrigated Area, HJ1A/1BCCD, Drought Index Difference Threshold

***Abstract:*** The increase in demand for agricultural products and population growth have led to water shortages, vigorous implementation of water-saving irrigation measures, and the development of accurate and efficient modern irrigated agriculture are long-term tasks for China's agricultural development. Irrigation management is one of the most important ways to implement the most stringent water management systems, and scientific irrigation management must be based on accurate and effective irrigation information. The traditional methods of information acquisition have the disadvantages of obtaining information, few monitoring points, time-consuming and laborious and long update period. This paper selects the application in the middle and upper reaches of the Yellow River, selects the HJIA // 1BCCD satellite data, and calculates and analyzes the distribution and changes of the vertical drought index and the revised vertical drought index in the two irrigation periods. The relationship between the threshold and the irrigated area determines the difference threshold. This paper calculates the irrigated area for both irrigations. Ground monitoring and statistics show that the results are reasonable. Based on the Landat TM data, a remote sensing irrigation area monitoring model based on the drought threshold is established, which can effectively and conveniently realize large-scale monitoring of the actual irrigation area. Provide technical support for real-time monitoring; provide a basis for effective integration of current irrigation status and scientific irrigation management decisions, thereby improving water use efficiency in irrigated areas and ensuring regional food security.

## 1. Introduction

The development of intelligent agriculture has promoted the development of agricultural irrigation technology. In the field of soil information collection, it is mainly to establish wireless sensor networks [1]. Information processing [2] is a prerequisite for growth in determining whether soil information meets irrigation conditions and ensures that the soil environment is optimal for the crop. Existing irrigation techniques [3] use a semi-automatic mode that typically requires manual observation of the agricultural environment and then irrigation. Some fields are over-irrigated and some fields are under-irrigated. With the development of the Internet of Things [4], the connection between people and things is possible. The development of intelligent agriculture is the only way to achieve agricultural modernization. It is necessary to develop intelligent irrigation systems [5] to overcome the problems of traditional agriculture. This is also the key to realizing agricultural irrigation and water saving, increasing effective irrigation area and agricultural output. The development of irrigation technology has significantly increased crop yield and stability, but it has also brought about negative effects such as soil salinization, groundwater pollution and rising groundwater [6]. At present, there are two main aspects of farmland irrigation research: irrigation and water and salt transportation, and water and fertilizer management models.

As the name suggests, remote sensing [7] is a distant perception, referring to the detection of non-direct contact integrated detection technology, recording the electromagnetic wave characteristics of the target from a distance, and revealing the characteristics and changes of the target through the target. In 1962, remote sensing technology was officially named "Remote Sensing" at the "Environmental Remote Sensing" conference held in the United States [8]. Since then, remote sensing has officially become a discipline. With the development of social science and technology and the launch of satellites, remote sensing technology has also developed rapidly in the 1960s. Such as information sources, information access and communication, information dissemination [9] and analytical processing [10], and information utilization. In addition, remote sensing technology has the advantages of all-weather, multi-time, multi-angle observation scale. Remote sensing technology can not only dynamically monitor and acquire surface and geological information, but also regularly monitor and acquire surface and geological information, so it is widely used in various fields. It has the following advantages: (1) Large range. Remote sensing technology can be used to detect most areas of high-altitude areas and even the Earth's surface, resulting in more efficient remote sensing data in less time. (2) Timeliness is strong. Since the Earth observation satellite system orbits the Earth, this feature can be used to repeatedly explore specific areas and update remote sensing data. In addition, through the comparative analysis of new and old remote sensing data in the same area, it is also possible to analyze the dynamic changes in the same area. (3) Data is more informative and comparable. Large-area information data can be obtained by remote sensing technology, which can directly reflect the distribution and state of various substances in the detection area. In addition, the collected data can be similar or identical by designing different remote sensing bands, imaging times and methods, and even data acquisition methods. According to the different needs of the target, it can be obtained by different remote sensing instruments, frequency bands and information acquisition means. (4) Quarters effort. Due to the different geographical conditions of the earth, human technology in some areas is still difficult to achieve. Aerospace remote sensing is not affected by ground environmental factors, and can acquire remote sensing data quickly and easily, which greatly saves manpower and material cost.

Monitoring is an important part of irrigation district management, a basic indicator of interest assessment, and an important indicator of regional water resources management [11]. Through real-time effective dynamic monitoring, the direction of irrigation water is quantitatively controlled to provide reasonable data for rational allocation, scheduling and management of irrigation water. Through scientific and effective management to improve water use efficiency and ensure the normal growth and production of irrigation water, starting from the improvement of irrigation information management level, using advanced technologies such as remote sensing to study irrigation area monitoring technology is of great significance to improve irrigation management level and water use efficiency. The application of remote sensing in irrigation districts mainly includes: (1) Obtain basic resource information of the irrigation area. It mainly includes land use and river systems, using multi-time remote sensing images to obtain information on land use change, thereby obtaining accurate distribution, crop planting area and irrigation area structure. According to the spectral characteristics of available water bodies, GLY absorbs the geometric characteristics of the mid-infrared band [12] and the river, and is recognized by high-resolution remote sensing factors such as rivers, lakes, diversion ditch, drainage ditch, etc., which is equivalent to the irrigation and drainage network of the irrigation area. (2) Estimate water resources in irrigated areas. It mainly includes two aspects: rainfall and crop water demand. Rainfall estimation [13] mainly uses visible light infrared and radar to obtain remote sensing images from Genting, analyzes cloud amount and microwave radiation factor to estimate instantaneous rainfall, and then uses meteorological radar and rainfall measurement station observation data for parametric calibration and accurate test to estimate instantaneous rainfall. Crop water requirements can be estimated by monitoring soil water content and corresponding thresholds can be set. Irrigation is carried out when the soil water potential is below a given lower threshold. (3) Irrigation area crop information. It mainly includes two aspects: crop disaster monitoring and crop growth monitoring. Crop disaster monitoring mainly includes disaster relief, drought and water shortage, and pests and diseases. For drought, internal errors can be monitored based on soil moisture content. At present, a variety of drought monitoring models have been applied to the monitoring of arid regions. See step (2) for details. Crop growth monitoring mainly refers to the early and middle stages of crop growth. The main method to monitor the whole process of crop growth and its late changes is to obtain the normalized vegetation index (NDVI) using red and near-infrared bands, which is a comprehensive reflection of crop growth. The principle is mainly that under the sunlight, the near-infrared band in the crop forms a reflection peak, and the visible band forms an absorption peak. When the growth state and vigor of the crop are different, the absorption and reflection abilities of the spectrum are also different, so the red band and the near infrared band can be used for monitoring. Crop growth (NDVI) is positively correlated with crop leaf area index and biomass. The higher the leaf area index, the higher the photo synthetically effective emission per unit area crop or the higher the number of crop spikes, the greater the value (NDVI). In addition, multi-time (NDVI) images are used for differential analysis and continuous classification of difference images. In order to monitor the growth of crops, pest and disease monitoring is mainly carried out in two aspects: crop infrared reflection anomaly and vegetation index decline. Remote sensing methods can be used to assess and classify large-scale crop pests and diseases, and the level of production management in irrigation districts is significantly improved. Remote sensing technology can provide a large amount of data for irrigation water management, and the analysis of these data can study the problem of uneven distribution of water resources. Water supply has different characteristics in terms of farming methods, irrigation intensity and crop growth. In the case of insufficient water supply, cultivation methods and irrigation intensity should be used to promote the effective use of water. The map combines remote sensing data and GIS to combine spectral information with topographic data (such as altitude, soil characteristics, and irrigation channel distribution). Differences in agricultural activities and other practices will increase the spectral variation of land in the irrigated area. In areas where there is a significant difference between crops that have a significant impact on spectral characteristics, the types of crops in the irrigated area are collected, the crops are classified and the irrigated areas are identified.

Some scholars used remote sensing, geographic information system and global positioning system technology to map the complete spatial distribution of the Zhangye Oasis main canal, branch channel and ditch in the middle reaches of the Heihe River. For the first time, the matching and visualization of the properties and spatial locations of the oasis irrigation channel system were realized. Some researchers applied the Gansu diversion irrigation project to the remote sensing and geographic information system. Through the analysis and research on the remote sensing data of the diversion project area, the types and distributions of landslides, debris flows and Quaternary sediments and geomorphology were analyzed. The project's geographic information system was established, and Quaternary geological and geomorphological maps, engineering layouts and irrigation patterns were drawn. Other scholars used remote sensing imagery and GIS technology to directly estimate the regional water evaporation in the Yakan River irrigation area, combined with the results of irrigation water evaporation experiments. It enables remote sensing maps to determine land use types, and GIS techniques are used to calculate areas of different land types and different groundwater depths, and calculate phreatic evaporation based on different land types.

Remote sensing has the characteristics of wide coverage, strong real-time and strong objectivity, which can provide data support for irrigation informationization construction. Firstly, based on the research significance of remote sensing technology in irrigation management, the demand for irrigation management information is analyzed. The shortage of irrigation management information collection in China was expounded and the remote sensing technology was compared with the traditional irrigation information collection method. At the same time, this paper introduces the application principle and method of remote sensing technology. In this paper, the Hetao Irrigation District in the middle and upper reaches of the Yellow River is used as the research area, and the HJ1A / 1B satellite data is mainly used. According to the vertical drought index before and after the transformation, the actual irrigation area is extracted by combining several measurement points on the ground. The crop structure is identified using high-resolution remote sensing images to obtain the actual irrigated area of the crop variety. Finally, the method extends to irrigation schedule monitoring. Satellite images such as landsat TM and fast birds are selected to identify irrigation channels, and based on topographic data, irrigation control zones are extracted using four adjacent regions of growth methods. The results show that real-time monitoring of irrigation and control areas is simple, input data is easy to obtain, and the results can be used as indicators for direct use of irrigation management services. In addition, based on the actual irrigated area extraction results for each subtype and the irrigation quota for each crop in the irrigated area, the actual irrigation amount is analyzed and compared to the flow monitoring information for the irrigated area. This provides a basic data for water-saving irrigation supervision.

## 2. Proposed Method

In order to better study the remote sensing monitoring technology of farmland irrigation, this paper introduces the relevant knowledge in the second part and lays a foundation for the subsequent experiments.

### 2.1. Nir-Red Spectral Feature Space

The leaf tissue has a strong absorption effect on blue-violet light and red light, and has a strong reflection effect on near-infrared rays. From red light to near-infrared (NIR), the reflectivity of bare ground is basically high, but the increase is not large, the higher the vegetation coverage, the greater the reflectance in near infrared band, and the smaller the reflectance in infrared band. In areas with high vegetation coverage, NIR light reflectance is closely related to leaf area index, leaf biomass and chlorophyll content. NDVI is suitable for early vegetation growth or low vegetation coverage monitoring. In images with uneven vegetation coverage, the triangles of the near-infrared vector set are very typical. The densest pixel is the top of the triangle: low red, high NIR. Different types of non-plant pixels, especially bare ground pixels. It is defined as the soil line in the lower right corner of the triangle. Dark, moist soil and water pixels appear at the left end of the soil line. The assumption of the slope of the soil line is defined: the amount of vegetation in the pixel is related to the Euclidean distance between the NIR red vector and its projection on the soil line, so the vegetation line is parallel to the soil line.

The results show that the short-wave infrared remote sensing Swir is more sensitive than the infrared remote sensing Red in vegetation moisture monitoring. Leaf area index (LAI), vegetation water content, and vegetation coverage all cause changes in Swir reflectivity. Swir has a high water absorption coefficient and is less affected by vegetation scattering, which can reach a certain vegetation depth in the canopy. The near-infrared band has a low water absorption rate, so SWIR is used as a monitoring band. It uses near-infrared as the reference band to establish the feature space, and the near-infrared feature space in the near-infrared band is more effective for surface moisture monitoring.

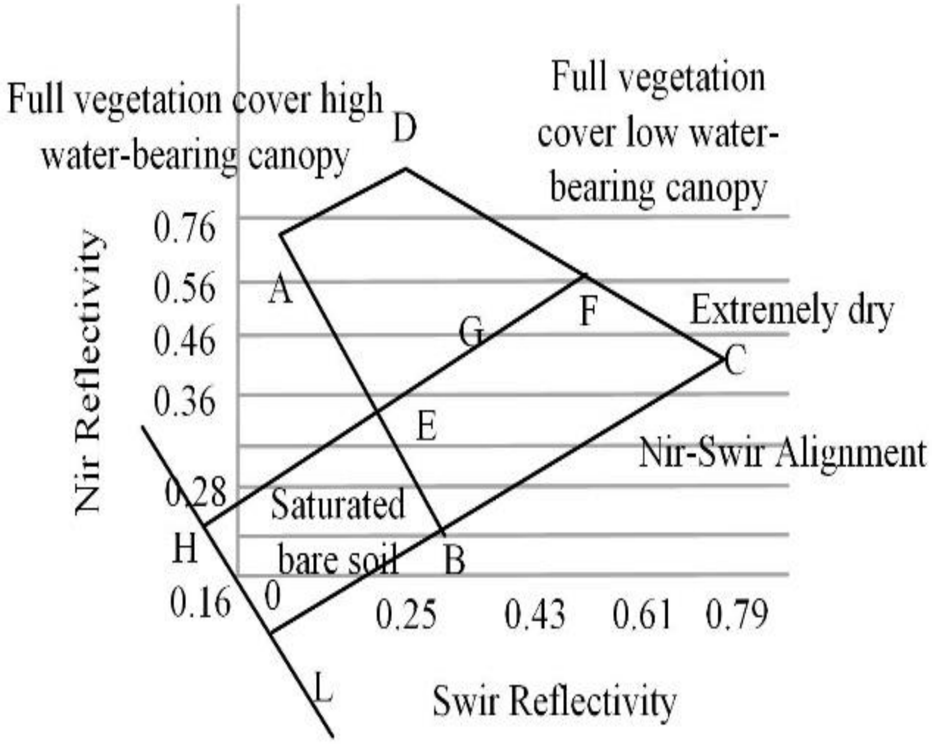


*Figure 1. Constructed $Nir-Swir$ spectral feature space curve*

In the feature space as shown Figure 1, the distance from the G point to the L line indicates the humidity of the object, and can also reflect the water stress of the vegetation. The further the distance, the more dry the object. Other reflective objects closer to the original vegetation also indicate a moister surface.

## 2.2. Drought Index Modeling

Vertical Drought Index $PDI$: The spectral feature space based on $Nir-Red$ near-infrared structure cannot only reflect the change of vegetation biomass, but also represent the change of soil water content. According to this rule, the vertical drought index ($PDI$) of bare land and low crop cover area is proposed. The $Nir-Red$ near-infrared feature space scattering pattern constructed from ETM data has a typical triangular distribution. The B-C is parallel to the soil reference line and the soil is gradually drying. A mathematical expression of the soil baseline can be obtained from the spatial feature map:

$$R_{nir} = M * R_{red} + I \tag{1}$$

Where $R_{red}$ is the reflectivity of the red band. $R_{nir}$ is the reflectance in the near infrared range. $M$ is the baseline slope of the soil. I is the intercept of the soil baseline at the y coordinate, and the normal to the origin of the coordinate perpendicular to the soil baseline $L$ is the normal equation of the equation. Point $E$ ($R_{red}, R_{nir}$) is selected from the $Nir-Red$ near-infrared triangular feature space, and the distance from point $E$ ($Rred, Rnir$) to line $L$ is the vertical drought index $PDI$. $PDI$ uses a distance $EF$ from any point $E$ ($Rred, Rnir$) in the $Nir-Red$ near-infrared triangular feature space to $L$ to characterize regional drought conditions.

$$PDI = \frac{1}{\sqrt{M^2+1}}\left(R_{red} + MR_{nir}\right) \tag{2}$$

$R_{red}$ and $R_{nir}$ are atmospherically corrected red and near infrared reflections. $M$ is the BC slope of the soil baseline. FL is perpendicular to the origin and soil baseline. Because the black body $PDI$ is zero, it only falls on the origin of the coordinates. The rest for any object with a certain reflectivity, the closer it is to the origin of the coordinate, the wet it is. In general, the closer $L$ is to the vertical distance of the line, the closer it is too wet areas such as water and wetlands. Where EF is close to zero and soil moisture is equal to or close to 1. The farther away from the vertical line, the area is drier and the EF is close to 1, so the soil moisture is close to or equal to zero. A soil moisture monitoring model ($SMMRS$) based on the spatial characteristics of $Nir-Red$ near-infrared spectra was established by subtracting the normalized value.

$$SMMRS = 1 - \frac{1}{\sqrt{M^2+1}}\left(R_{red} + MR_{nir}\right) \tag{3}$$

Modified drought index correction $MPDI$: This paper uses the $fv$ calculation method of vegetation coverage proposed by Baret. Vegetation coverage and surface vegetation coverage are important parameters of vegetation canopy. The vegetation adjustment function $fv$ is calculated using the close relationship between vegetation and vegetation spectral indices.

$$\begin{cases} fv = \left(\dfrac{NDVI - NDVI_S}{NDVI_V - NDVI_S}\right)^2 \\ fv = 1 - \left(\dfrac{NDVI - NDVI_S}{NDVI_V - NDVI_S}\right)^{0.6175} \end{cases} \tag{4}$$

In equation (4), $NDVI$ and $NDVI_V$ represent the $NDVI$ values for intact vegetation cover and bare land, respectively. These two values are obtained by continuous imaging of a single image or satellite image. $NDVI_S$ and $NDVI_V$ can be adjusted based on the geographic and temporal characteristics of the full vegetation pixels and bare pixels. Since the ratio index can minimize atmospheric effects, the $NDVI$ scale power function method can be used to reduce the effects of atmospheric disturbances. Assuming that the pixel consists of two terminal elements (bare land and vegetation), the mixed pixel reflectivity with $R_i$ can be identified as a comprehensive linear function of vegetation to soil ratio.

$$R_i = f_v R_{v,i} + \left(1 - f_v\right) R_{s,i} \tag{5}$$

In equation (5), $R_{v,i}$ and $R_{s,i}$ represent the reflections of vegetation and soil in the mixed pixels. By deforming the formula, the soil reflectivity $R_{s,i}$ can be obtained. Finally get:

$$MPDI = \frac{R_{red} + MR_{nir} - fv\left(R_{red,v} + MR_{nir,v}\right)}{(1-fv)\sqrt{M^2+1}} \tag{6}$$

Short-wave infrared vertical water loss index ($SPSI$): The $Nir-Swir$ spectral feature space scatter plot constructed from $ETM+$ data can be used to obtain the $Nir-Swir$ soil baseline BC after spatial analysis, ie:

$$R_{nir} = M * R_{swir} + I \tag{7}$$

In Equation (7), $R_{swir}$ and $R_{nir}$ are the atmospheric corrected short-wave infrared and near-infrared reflectivity, $M$ is the slope of the $N_{ir} - S_{wir}$ soil line, and $I$ is the intercept of the $Nir-Swir$ soil line ordinate. The degree of stress in the crop is described by the distance from any point on the $Nir-Swir$ feature space to the $L$ line. And the vegetation water index based on the $Nir-Swir$ feature space, namely $SPSI$:

$$SPSI = \frac{1}{\sqrt{M^2+1}}\left(R_{swir} + MR_{nir}\right) \tag{8}$$

In the Equation (8), $R_{swir}$ and $R_{nir}$ are reflectances of the $Swir$ and $Nir$ bands corrected by the atmosphere. $M$ is the baseline $BC$ slope of the Soil line soil. $FL$ is a perpendicular to the origin and perpendicular to the soil line.

### 2.3. Remote Sensing Irrigation Area Monitoring Model based on the Difference National Value of Drought Index

The direct drought index can reflect changes in soil moisture, but it cannot be used to obtain quantitative indicators of irrigation areas. According to the change law of soil moisture increase after irrigation, the soil moisture increased, the drought index decreased, the soil moisture continued to decrease, and the drought index continued to rise. Based on this principle, an irrigation monitoring model based on the difference threshold of drought index is established, and its structure is shown in Equation (9):

$$\begin{cases} I_1 = PDI_{t1} - PDI_{t2} \\ I_2 = MPDI_{t1} - MPDI_{t2} \end{cases} \tag{9}$$

The drought index is reduced by two levels of image calculations. When the current drought index is greater than the late drought index, it means that there is irrigation during this period; otherwise it means no irrigation. Equation (9) represents the difference calculated based on the vertical drought index and the difference calculated based on the corrected vertical drought index. $I$ represents the extent to which the pixel area is affected by irrigation. The smaller $I$ is, the worse the irrigation effect will be. When the threshold is very small, it can be considered that there is no irrigation in the pixel area. $PDI$ before irrigation is $PDI_{t1}$, and the $PDI$ after irrigation is $PDI_{t2}$. The larger the PDI, the more severe the drought is. $MPDI_{t1}$ is $MPDI$ before irrigation and $MPDI_{t2}$ is $MPDI$ after irrigation. The larger the $MPDI$, the more severe the drought is. In theory, as long as there is a positive difference in the drought index, it is possible to irrigate. However, due to the accuracy of the remote sensing interpretation of the drought index and the differences in the acquisition conditions of the two images, the difference in the drought index has a certain invalid range. Therefore, it is necessary to set the difference threshold to eliminate the influence of interference factors.

## 3. Experiments

### 3.1. Selection of Remote Sensing Data of Actual Irrigation Area

The main research contents of remote sensing monitoring in actual irrigation area include crop planting structure identification, five-round actual irrigation area extraction in Bawei Village, autumn irrigation data selection in Hetao Irrigation District in 2017 and actual area extraction of Hetao Irrigation District in August 2018. A total of 8 HJ1A / 1B CCD images from May to September were selected to realize remote sensing monitoring of 5 actual irrigation areas in Bawei Village. From September to November 2018, four HJ1A / B CCD images were used as river irrigation areas. The planting structure of the crop was determined using full-color multispectral data from the Resource 3 satellite and the Tianhui 1 satellite. The parameters and time of the data used are shown in Table 1 below.

*Table 1. Main parameters of satellites used for remote sensing monitoring of actual irrigated area*

| Satellite | Sensor | Number of bands | Band (um) | Spatial resolution (m) | Time resolution (d) | Width (km) | Selected data |
|---|---|---|---|---|---|---|---|
| HJ1A/1B | Multispectral | 4 | 0.43-0.52<br>0.52-0.60<br>0.63-0.69<br>0.76-0.90 | 30 | 2 | 700 | 2017 river set 12 scenes 2018/8/2 view |
| Resource number three | Panchromatic | 1 | 0.5-0.80<br>0.45-0.52<br>0.52-0.59<br>0.63-0.69<br>0.77-0.90 | 2.1 | 5 | 51 | 2018/6/13 |
| | Multispectral | 4 | | 6 | 5 | 51 | |
| Tianhui 1 | Panchromatic | 4 | 0.51-0.79<br>0.43-0.52<br>0.52-0.61<br>0.61-0.69<br>0.76-0.90 | 2 | 58 | 60 | 2018/9/1 |
| | Multispectral | | | 10 | 58 | 60 | |
| High score one | Multispectral | 4 | 0.45-0.52<br>0.52-0.59<br>0.63-0.69<br>0.77-0.89 | 16 | 4 | 800 | 2018/8/3<br>2018/8/11 |

### 3.2. Difference Threshold Selection

There are 10 survey sites in the study area to record the irrigation conditions at the survey site. These 10 locations include land use types such as plantations and wasteland. Therefore, it can be assumed that the difference in image acquisition conditions in the same region is uniform. In the case of rainfall during irrigation, the impact of rainfall on plantation and wasteland MPDI is the same. The MPDI difference threshold is adjusted according to the MPDI difference of 10 measurement points, so that the extraction result of the irrigation area is consistent with the measurement results of the 10 measurement points. The area extracted by this threshold is the actual irrigated area of the current round of irrigation.

Taking the first round of irrigation in 2018 as an example, the MPDI differential threshold analysis process is illustrated. The MPDI differences of 10 measurement points were analyzed, including 3 single measurement points, and the MPDI differences were 1.46, 1.55 and 1.52, respectively. The remaining seven locations were irrigation sites with MPDI differences of 1.61, 1.72, 1.68, 1.52, 1.62, 1.80, and 1.78, respectively. Therefore, the MPDI difference threshold extracted in the current round of irrigation area is 1.55, which can achieve the highest consistency between the extraction result and the measurement point. $I = 1.55$, the actual irrigated area is 1409 acres. The above steps are used to analyze the actual irrigated area of the remaining four rounds of irrigation in 2018. The $I$ values are 0.68, 1.64, 1.78 and 1.82, and the irrigated area is 942 acre, 1827 acre, 1778 acre and 1814 acre.

### 3.3. Crop Planting Structure Identification

The crop variety identification data is the full-color and multi-spectral fusion data of Resource No. 3 on June 13, 2018. The geographical area of the study area is 40°24'4.64“N~40°25'12.85”N, 107°1'7.98 "E~107°3'3.62" E. The key steps in SVM classification are: training sample library creation, target template creation, target extraction and post-processing. Based on field survey data, seven mixed training samples were identified: wheat, sunflower, corn, summer miscellaneous, building, pure water, and wood, bare land, and so on. Their number is shown in Figure 2. From the figure we can see that the corresponding numbers are 20, 23, 17, 25, 15, 9, 16, and 15, when collecting samples, try to select mixed pixels in order to bias the selected training samples to a category.

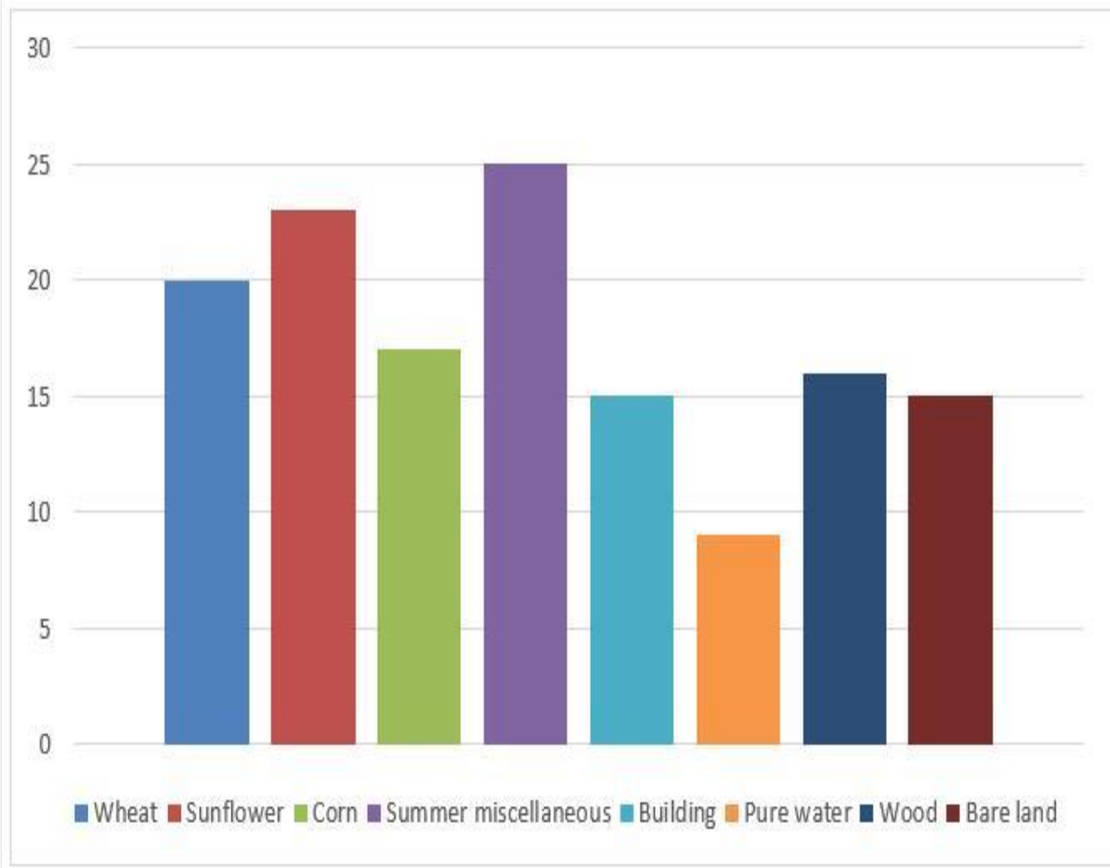


*Figure 2. The corresponding number of training samples*

### 3.4. Irrigation Schedule Monitoring

Based on the MPDI differential threshold, the actual irrigation district extraction model is only applicable to small areas of the dam village. In order to verify the validity of the model, it is necessary to further demonstrate the model at different times and in larger spaces. In summary, the monitoring of autumn water back irrigation in Hetao Irrigation District is not only an urgent need for pattern detection, but also an urgent need for irrigation district management. During the autumn and winter rains of 2018, four images of good environmental stars were selected and collected on September 15, September 28, October 13, and October 28. Taking September 15 as the time node before irrigation, the extracted irrigation area is input into the MPDI differential calculation model according to the difference of MPDI before and after irrigation, and the threshold is analyzed by combining the ground measurement points. Finally, the actual irrigation area at three time points is extracted based on the threshold.

## 4. Discussion

### 4.1. Analysis of the Relationship between MPDI and Soil Water Content

The correlation between MPDI and soil water content was first studied. There are 20 soil monitoring points in the 2023 mu test site of Bawei Village, Qingkou County, and the soil moisture content is measured 4 times per month. Figure 3 shows the use of soil moisture monitoring points from May to August 2018 to select the average soil water content data at a depth of 0-20 cm corresponding to the 208 observation points, consistent with the image data of June 25, 2018. In addition, soil moisture content and MPDI index values measured at the same coordinate point in the 10-stage image were compared. The result is shown in Figure 4.

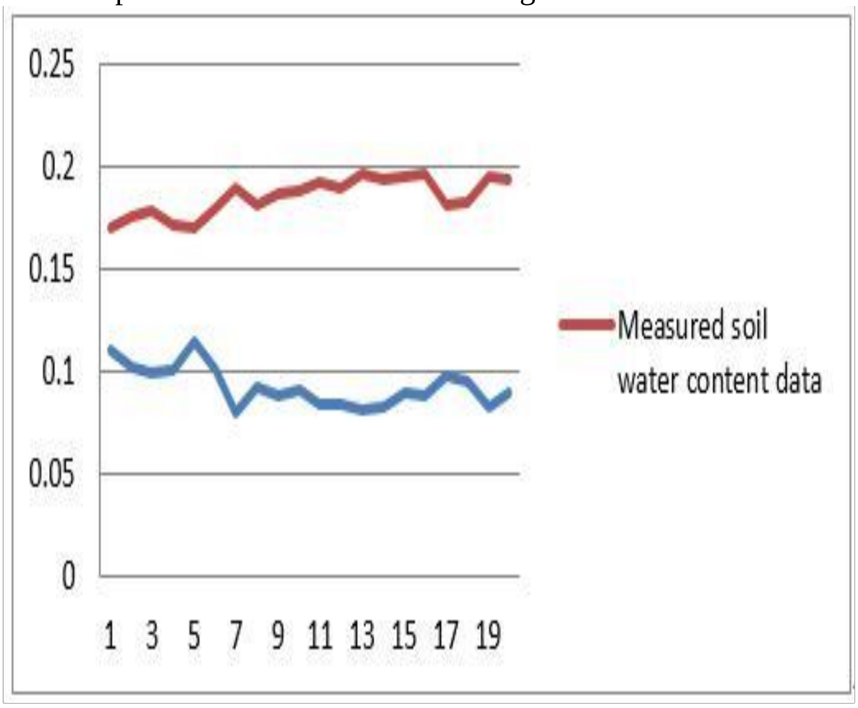


*Figure 3. Soil moisture content and corresponding MPDI values of 20 ground monitoring sites on June 25*

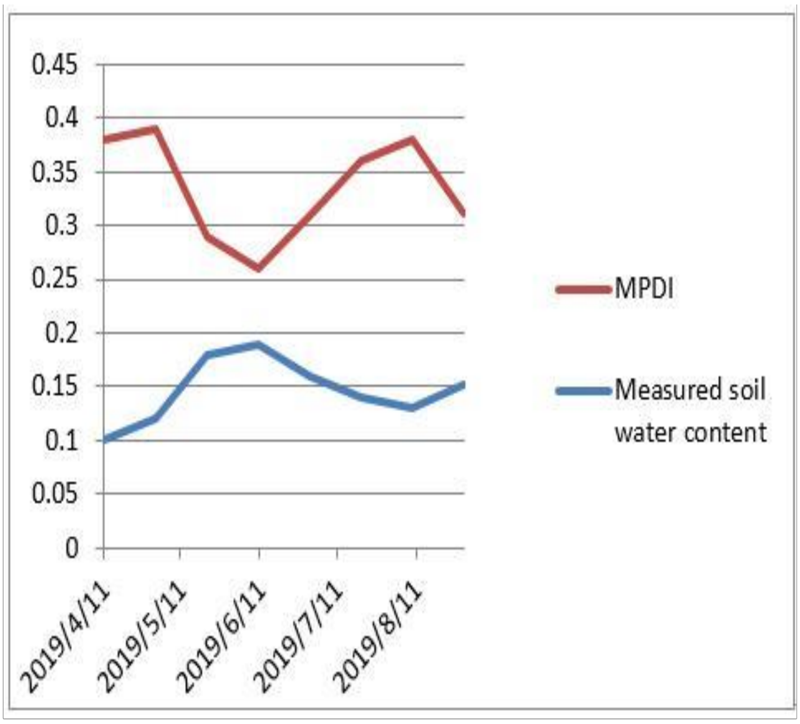


*Figure 4. Changes in MPDI and soil water content at the same location at different time points*

As can be seen from Figures 3 and 4, the larger the MPDI in terms of time and space, the smaller the measured soil moisture content. MPDI is negatively linearly correlated with the measured soil water content. R2 is 0.883, which indicates that MPDI can better reflect soil water content.

### 4.2. Analysis of the Results of Five Rounds of Actual Irrigation Area

Combined with the identification of crop planting structure, the actual irrigated area of crops in 5 rounds of the dam village was obtained, as shown in Table 2.

*Table 2. Actual irrigated area of five rounds of water crops in 2018*

| Crop type | First round (acre) | Second round (acre) | Third round (acre) | Fourth round (acre) | Fifth round (acre) |
|---|---|---|---|---|---|
| Wheat | 111.8 | 41.9 | 140.5 | 141.5 | 130.65 |
| Sunflower | 522.0 | 402.1 | 736.0 | 706.8 | 713.43 |
| Corn | 254.2 | 241.5 | 381.5 | 382.8 | 341.73 |
| Other | 521.7 | 257.2 | 568.9 | 551.6 | 627.66 |
| Total | 1409.7 | 942.7 | 1821.9 | 1777.7 | 1813.4 |

Table 2 shows the five-round irrigated area in 2018 and the spatial distribution of each crop, which visually shows the irrigation effect. In addition, wheat entered the harvest season in August and no irrigation in the fifth round. However, 130.65 acres of wheat irrigation monitoring reflects the inconsistency between the irrigation system and the actual operation of the farmers.

### 4.3. Analysis of Water Consumption

The extraction range is superimposed on the crop planting structure, and the area of each irrigated crop is multiplied by the crop quota to obtain the estimated amount of water, and compared with the water consumption statistics of the demonstration area.

The first round: the error between the amount of water calculated in the first round and the actual amount of water is -23.29%.

| Crop type | Area (acre) | Quota ($m^3$/acre) | Estimated water volume ($m^3$) | Statistical water volume ($m^3$) | Error (%) |
|---|---|---|---|---|---|
| Wheat | 111.8 | 80 | 8941.6 | | |
| Sunflower | 522.0 | 80 | 41763.2 | | |
| Corn | 254.2 | 50 | 12712.5 | | |
| Summer Miscellaneous | 521.7 | 64 | 33390.1 | | |
| Total | 1409.8 | | 96807.4 | 126200 | -23.29 |

The second round: the error between the amount of water calculated in the second round and the actual amount of water is 32.07%.

| Crop type | Area (acre) | Quota ($m^3$/acre) | Estimated water volume ($m^3$) | Statistical water volume ($m^3$) | Error (%) |
|---|---|---|---|---|---|
| Wheat | 41.9 | 45 | 1885.4 | | |
| Sunflower | 402.1 | 50 | 20103.9 | | |
| Corn | 241.5 | 40 | 9660.6 | | |
| Summer Miscellaneous | 257.2 | 50 | 12857.6 | | |
| Total | 942.6 | | 44507.5 | 33700 | 32.07 |

The third round: the error between the amount of water calculated in the third round and the actual amount of water is 29.77%.

| Crop type | Area (acre) | Quota ($m^3$/acre) | Estimated water volume ($m^3$) | Statistical water volume ($m^3$) | Error (%) |
|---|---|---|---|---|---|
| Wheat | 140.5 | 76 | 10674.9 | | |
| Sunflower | 736.0 | 70 | 51522.1 | | |
| Corn | 381.5 | 75 | 28611.8 | | |
| Summer Miscellaneous | 568.9 | 63 | 35842.6 | | |
| Total | 1826.9 | | 126651.4 | 97600 | 29.77 |

The fourth round: the water quantity verification is as follows, the error between the water quantity calculated in the fourth round and the actual water quantity is -0.76%.

| Crop type | Area (acre) | Quota ($m^3$/acre) | Estimated water volume ($m^3$) | Statistical water volume ($m^3$) | Error (%) |
|---|---|---|---|---|---|
| Wheat | 141.6 | 60 | 8496.4 | | |
| Sunflower | 701.8 | 62 | 43513.0 | | |
| Corn | 382.8 | 60 | 22970.6 | | |
| Summer Miscellaneous | 551.6 | 60 | 33093.8 | | |
| Total | 1777.8 | | 108073.92 | 108900 | -0.76 |

The fifth round: the error between the amount of water calculated in the fifth round and the actual amount of water is -14.53%.

| Crop type | Area (acre) | Quota ($m^3$/acre) | Estimated water volume ($m^3$) | Statistical water volume ($m^3$) | Error (%) |
|---|---|---|---|---|---|
| Wheat | 130.6 | | | | |
| Sunflower | 713.4 | 62 | 44232.8 | | |
| Corn | 341.7 | 65 | 22212.3 | | |
| Summer Miscellaneous | 627.7 | 60 | 37659.6 | | |
| Total | 1813.5 | | 104104.6 | 121800 | -14.53 |

The amount of water used can be estimated based on the actual irrigated area and the irrigation quota of the crop type. The quantitative use of crop irrigation water can reflect the irrigation effect and water efficiency. The results show that 2450127 acres will be irrigated before September 28, 4461516 acres will be irrigated before October 13, and 10894527 acres will be irrigated before October 28. The results of remote sensing monitoring directly reflect the spatial distribution and irrigation process of the irrigation area. In 2018, the administrative department of Hetao Irrigation District plans to irrigate more than 2 million mu by the end of September and early October. The irrigation area will exceed 4 million mu in mid-October, and the irrigation amount will exceed 10 million mu at the end of October. The monitoring results of remote sensing irrigation showed that the expected results were completed in the autumn of 2018 and have been achieved.

### 4.4. Real-Time Irrigated Area Remote Sensing Monitoring Verification

From May to August 2018, the average water content of 20 soil water contents in Batun Village is 0-20 cm, which is caused by irrigation at various points in a certain period of time. The actual irrigation range extracted is compared to the measured soil moisture point irrigation conditions, which can be verified on a point scale. Due to the lack of ground monitoring sites in September, the fifth round of irrigation did not participate in the verification. The results of one to four rounds of irrigation verification are as follows:

The accuracy of the first round of irrigation and the measured results at the point reached 90%.

| Point number | 1 | 2 | 3 | 4 | 5 | 6 | 7 | 8 | 9 | 10 |
|---|---|---|---|---|---|---|---|---|---|---|
| Measured | Irrigation | Irrigation | Irrigation | Irrigation | Irrigation | Irrigation | No irrigation | Irrigation | Irrigation | Irrigation |
| Estimate | Irrigation | Irrigation | Irrigation | Irrigation | Irrigation | Irrigation | Irrigation | No irrigation | Irrigation | Irrigation |
| Point number | 11 | 12 | 13 | 14 | 15 | 16 | 17 | 18 | 19 | 20 |
| Measured | Irrigation | Irrigation | Irrigation | Irrigation | Irrigation | Irrigation | Irrigation | Irrigation | Irrigation | Irrigation |
| Estimate | Irrigation | Irrigation | Irrigation | Irrigation | Irrigation | Irrigation | Irrigation | Irrigation | Irrigation | Irrigation |

The accuracy of the second round of irrigation range and the measured results at the point reached 80%.

| Point number | 1 | 2 | 3 | 4 | 5 | 6 | 7 | 8 | 9 | 10 |
|---|---|---|---|---|---|---|---|---|---|---|
| Measured | Irrigation | Irrigation | Irrigation | Irrigation | Irrigation | Irrigation | Irrigation | Irrigation | Irrigation | Irrigation |
| Estimate | No irrigation | Irrigation | Irrigation | Irrigation | Irrigation | Irrigation | Irrigation | Irrigation | No irrigation | Irrigation |
| Point number | 11 | 12 | 13 | 14 | 15 | 16 | 17 | 18 | 19 | 20 |
| Measured | Irrigation | Irrigation | Irrigation | Irrigation | Irrigation | Irrigation | No irrigation | No irrigation | No irrigation | No irrigation |
| Estimate | No irrigation | Irrigation | Irrigation | Irrigation | No irrigation | Irrigation | No irrigation | No irrigation | No irrigation | No irrigation |

The accuracy of the third round of irrigation range and the measured results on the point reached 85%.

| Point number | 1 | 2 | 3 | 4 | 5 | 6 | 7 | 8 | 9 | 10 |
|---|---|---|---|---|---|---|---|---|---|---|
| Measured | Irrigation | Irrigation | Irrigation | Irrigation | Irrigation | Irrigation | Irrigation | Irrigation | Irrigation | Irrigation |
| Estimate | No irrigation | Irrigation | Irrigation | Irrigation | Irrigation | No irrigation | Irrigation | Irrigation | Irrigation | Irrigation |
| Point number | 11 | 12 | 13 | 14 | 15 | 16 | 17 | 18 | 19 | 20 |
| Measured | Irrigation | Irrigation | Irrigation | Irrigation | Irrigation | Irrigation | Irrigation | Irrigation | Irrigation | Irrigation |
| Estimate | Irrigation | Irrigation | Irrigation | Irrigation | Irrigation | Irrigation | Irrigation | Irrigation | Irrigation | No irrigation |

The accuracy of the fourth round of irrigation range and the measured results on the point is 85%.

| Point number | 1 | 2 | 3 | 4 | 5 | 6 | 7 | 8 | 9 | 10 |
|---|---|---|---|---|---|---|---|---|---|---|
| Measured | Irrigation | Irrigation | Irrigation | Irrigation | Irrigation | Irrigation | Irrigation | Irrigation | Irrigation | Irrigation |
| Estimate | Irrigation | Irrigation | Irrigation | No irrigation | Irrigation | Irrigation | Irrigation | No irrigation | Irrigation | Irrigation |
| Point number | 11 | 12 | 13 | 14 | 15 | 16 | 17 | 18 | 19 | 20 |
| Measured | Irrigation | Irrigation | Irrigation | Irrigation | Irrigation | Irrigation | Irrigation | Irrigation | Irrigation | Irrigation |
| Estimate | Irrigation | Irrigation | Irrigation | Irrigation | Irrigation | No irrigation | Irrigation | No irrigation | Irrigation | Irrigation |

The verification results of four rounds of soil water content show that the accuracy of remote sensing monitoring irrigation can reach more than 85%.

### 4.5. Irrigation Schedule Monitoring Verification

Based on the survey data of 10 soil moisture monitoring stations in Hetao Irrigation District, the accuracy of irrigation extraction in three periods of autumn irrigation was tested. See Table 3 for details. Compared with the results of comparative survey and remote sensing monitoring, the consistency between them can reach more than 80%. Inconsistent points include irrigation surveys, irrigation surveys, and unirrigated irrigation surveys.

*Table 3. Irrigation progress monitoring verification*

| Public opinion monitoring site name | September 28 | October 13 | October 28 |
|---|---|---|---|
| Dam | Error | Correct | Error |
| Three bridges | Correct | Correct | Correct |
| Four brakes | Correct | Correct | Correct |
| Red star | Correct | Error | Error |
| Xinhua Institute | Correct | Correct | Correct |
| Taal Lake | Error | Correct | Correct |
| Lianfeng | Correct | Correct | Correct |
| Heshengxiang | Correct | Correct | Correct |
| Changsheng Township | Correct | Correct | Correct |
| Xin'an Town | Correct | Correct | Correct |

With the support of the project, GF-1 satellite data docking based on GF-1 irrigation area monitoring was carried out. The GF-1 data of the two scenarios and the environmental star data of the same period were used to monitor and compare the actual irrigated area of Qikou County in Hetao Irrigation District in August. From the perspective of visual interpretation, the 16-meter multispectral data of the high-resolution satellite 1 is larger than the environmental star multi-spectral (30-meter) image, with obvious feature boundaries, clear texture and rich texture information, and building layers. Large building texture information, wide roads and canal systems are all recognizable, and smaller objects are difficult to identify. The two satellite data obtained are input into the MPDI differential calculation model, and the threshold is extracted by threshold analysis to extract the irrigation area. According to the data of Peak No.1, the irrigation area is 18,500 mu, and the environmental star extraction area is 24,189 mu. The results show that there are differences in the area of the two methods, and the extraction effect of environmental stars is greater than that of GF-1, but the spatial overlap is very high. According to the statistics of the Dongfeng Irrigation District Management Office of Hetao Irrigation District, the amount of irrigation water in the first half of August was about 20,000 mu, which is close to the two monitoring data.

## 5. Conclusion

At present, the world's irrigated area is 2.7×108hm2, accounting for only 17% of the world's total arable land, but crop production accounts for one-third of global food production. Irrigation technology has a huge impact on global food. In China, agriculture in most areas relies on irrigation. The area of irrigated area accounts for less than 40% of the total area of cultivated land, and grain production accounts for more than 74%. Especially large and medium-sized irrigated areas play an important role in Chinese agriculture. China is a country with a severe shortage of water resources. Per capita water resources are only one-fourth of the world average. However, water shortages and wastes coexist in agriculture. The efficiency of natural precipitation and irrigation is very low. Vegetation and shallow groundwater have a large impact. Reduced irrigation efficiency also means that large amounts of irrigation water flow back into rivers and aquifers, and irrigation in some areas is excessively concentrated, further leading to stagnant water and salinization. As the population increases, the total demand for food and other agricultural products will continue to grow. By 2030, China's total grain demand is expected to reach 700 million tons, and the irrigated area must reach 900 million acres to meet agricultural production needs. According to the current water consumption, agricultural demand will be reduced by 60-70 billion cubic meters. Judging from the actual situation of severe water shortage in China, it is impossible to alleviate the shortage of agricultural water by simply adding new water sources. From an economic point of view, only a few regions in China can rationally develop new water sources. The cost of developing new water sources is much higher than the cost of water conservation. Therefore, it is unrealistic to solve agricultural water problems such as cross-basin water diversion through the above methods. As a result, most regions must meet new water needs through potential savings and improved irrigation management.

Remote sensing monitoring is an important part of irrigation district management, a basic indicator of interest evaluation, and an important indicator of regional water resources management. Through real-time effective dynamic monitoring, the direction of irrigation water is quantitatively controlled to provide reasonable data for rational allocation, scheduling and management of irrigation water. Improve water use efficiency through scientific and effective management to ensure the normal growth and production of irrigation water. Therefore, starting from the improvement of irrigation information management level, using advanced technologies such as remote sensing to study irrigation area monitoring technology is of great significance to improve irrigation management level and water use efficiency.

## Funding

This article is not supported by any foundation.

## Data Availability

Data sharing is not applicable to this article as no new data were created or analysed in this study.

## Conflict of Interest

The author states that this article has no conflict of interest.

## References

*[1] Kurt, S., Yildiz, H. U., Yigit, M., Tavli, B., & Gungor, V. C. (2016) "Packet Size Optimization in Wireless Sensor Networks for Smart Grid Applications", IEEE Transactions on Industrial Electronics, 64(3), pp. 2392-2401. https://doi.org/10.1109/TIE.2016.2619319*

*[2] Ford, J. D. (2017) "Treatment Implications of Altered Affect Regulation and Information Processing Following Child Maltreatment", Psychiatric Annals, 35(5), pp. 410-419. https://doi.org/10.3928/00485713-20050501-07*

*[3] Akcay, M., Arslan, H., Mese, M., Durmus, N., & Capar, I. D. (2017) "Effect of Photon-Initiated Photoacoustic Streaming, Passive Ultrasonic, and Sonic Irrigation Techniques on Dentinal Tubule Penetration of Irrigation Solution: A Confocal Microscopic Study", Clinical oral investigations, 21(7), pp. 2205-2212. https://doi.org/10.1007/s00784-016-2013-y*

*[4] Dastjerdi, A. V., & Buyya, R. (2016) "Fog Computing: Helping the Internet of Things Realize*

*Its Potential", Computer, 49(8), pp. 112-116. https://doi.org/10.1109/MC.2016.245*

*[5] Kponyo, J. J., Opare, K. A. B., Abdul-Rahman, A., & Agyemang, J. O. (2019) "An Intelligent Irrigation System for Rural Agriculture", Agriculture. International, 5(3), pp. 75-81. https://doi.org/10.11648/j.ijaas.20190503.13*

*[6] Xiang, X., Li, Q., Khan, S., Khalaf, O.I. Urban water resource management for sustainable environment planning using artificial intelligence techniques. Environmental Impact Assessment Review, 2021, 86, 106515 https://doi.org/10.1016/j.eiar.2020.106515*

*[7] Zhang, L., Zhang, L., & Du, B. (2016) "Deep learning for remote sensing data: A Technical Tutorial on the State of the Art", IEEE Geoscience and Remote Sensing Magazine, 4(2), pp. 22-40. https://doi.org/10.1109/MGRS.2016.2540798*

*[8] Adil, M., Khan, M. K., Jamjoom, M., & Farouk, A. (2021). MHADBOR: AI-enabled Administrative Distance based Opportunistic Load Balancing Scheme for an Agriculture Internet of Things Network.IEEE Micro. https://doi.org/10.1109/MM.2021.3112264*

*[9] Lokot, T., & Diakopoulos, N. (2016) "News Bots: Automating News and Information Dissemination on Twitter", Digital Journalism, 4(6), pp. 682-699. https://doi.org/10.1080/21670811.2015.1081822*

*[10] Giannopoulos, K., & Boutsinas, B. (2016) "Tourism Satellite Account Support using Online Analytical Processing", Journal of Travel Research, 55(1), pp. 95-112. https://doi.org/10.1177/0047287514538836*

*[11] Selçuk Topal, Ferhat Tas, Said Broumi, Oguz Ayhan Kirecci, Applications of Neutrosophic Logic of Smart Agriculture via Internet of Things, International Journal of Neutrosophic Science, 2020, Vol. 12, No. 2, pp: 105-115 (Doi : https://doi.org/10.54216/IJNS.120205)*

*[12] Guo, Q., Pospischil, A., Bhuiyan, M., Jiang, H., Tian, H., Farmer, D. & Xia, Q. (2016) "Black Phosphorus Mid-Infrared Photodetectors with High Gain", Nano Letters, 16(7), pp. 4648-4655. https://doi.org/10.1021/acs.nanolett.6b01977*

*[13] Thompson, E. J., Rutledge, S. A., Dolan, B., Thurai, M., & Chandrasekar, V. (2018) "Dual-Polarization Radar Rainfall Estimation over Tropical Oceans", Journal of Applied Meteorology and Climatology, 57(3), pp. 755-775. https://doi.org/10.1175/JAMC-D-17-0160.1*